Drag of buoyant vortex rings

Ahmadreza Vasel-Be-Hagh,[*] Rupp Carriveau,[†] and David S.-K. Ting[‡]
Turbulence and Energy Laboratory, Lumley Centre for Engineering Innovation, University of Windsor, Ontario N9B 3P4, Canada

John Stewart Turner[§]
Research School of Earth Sciences, Australian National University, Canberra, ACT 0200, Australia
(Received 22 June 2015; published 30 October 2015)

Extending from the model proposed by Vasel-Be-Hagh *et al.* [J. Fluid Mech. **769**, 522 (2015)], a perturbation analysis is performed to modify Turner's radius by taking into account the viscous effect. The modified radius includes two terms; the zeroth-order solution representing the effect of buoyancy, and the first-order perturbation correction describing the influence of viscosity. The zeroth-order solution is explicit Turner's radius; the first-order perturbation modification, however, includes the drag coefficient, which is unknown and of interest. Fitting the photographically measured radius into the modified equation yields the time history of the drag coefficient of the corresponding buoyant vortex ring. To give further clarification, the proposed model is applied to calculate the drag coefficient of a buoyant vortex ring at a Bond number of approximately 85; a similar procedure can be applied at other Bond numbers.

DOI: 10.1103/PhysRevE.92.043024 PACS number(s): 47.32.C−, 47.10.A−, 47.55.dd, 47.55.P−

I. INTRODUCTION

Vortex rings are categorized into buoyant and nonbuoyant groups depending on whether they contain a fluid lighter than the surrounding fluid. Drag of nonbuoyant vortex rings has been extensively studied by Gan *et al.* [1]; however, there is a dearth of published research concerning the drag of buoyant vortex rings—although their other overall properties (e.g., circulation, radius, rise velocity, stability, lifetime, etc.) have been widely investigated [2–5]. One of the earliest analytical theories about buoyant vortex rings, also called vortex ring bubbles or toroidal bubbles, was developed by Turner [2], predicting that a rising buoyant vortex ring expands radially as

$$R_T = \left(R_0^2 + \frac{Ft}{\pi\Gamma}\right)^{1/2}, \tag{1}$$

where R_T, namely Turner's radius, is the radius of the toroid at time t, R_0 is the initial radius of the toroid, Γ is the circulation, and F is defined as $g\,\Omega(\rho\text{-}\rho')/\rho$ in which Ω is the volume of the toroid, ρ is density of water, and ρ' is density of air. Equation (1) was devised under two fundamental assumptions:

(i) As sketched in Fig. 1, a region of rotational flow rising along with the vortex ring was postulated. Turner [2] assumed that no vorticity diffuses across the boundary of this region B; that is, no vorticity is lost to a wake.

(ii) Vorticity generated on the surface of the vortex ring was assumed to be confined within a region which never extends to the symmetry axis ($O\,O'$ in Fig. 1). In other words, no vorticity is canceled due to diffusion across the axis of symmetry.

These assumptions also underlie some later theoretical and numerical analyses, such as those of Walters and Davidson [4] and Pedley [5]. In view of Turner's assumptions, circulation of buoyant vortex rings remains constant since vorticity is constant and the viscous effect is negligible since there is no momentum loss in a viscous wake. In other words, buoyancy is assumed to be the only effective force on the buoyant vortex rings. In a recent study [6], we proposed a drag-based model to take into account the effect of a viscous force in addition to the effect of a buoyancy force on the radial expansion of buoyant vortex rings. The idea was inspired by the model proposed by Sullivan *et al.* [7] for nonbuoyant vortex rings (also see Hershberger *et al.* [8]). Our model was developed on the basis of a force balance equation according to which the impulse of a buoyant vortex ring increases under the action of buoyancy while the drag force causes the impulse to decrease as given by

$$\frac{dP}{dt} = F_B - 2\pi\rho a R C_d V^2, \tag{2}$$

where F_B is the buoyancy force, C_d is the drag coefficient, V is the rise velocity, a is the radius of the core, and R is the radius of the toroid. Consider the following classical equations, respectively, for the impulse P and rise velocity V of vortex rings

$$P = \rho\Gamma\pi R^2 \tag{3}$$

$$V = \frac{\Gamma}{4\pi R}\left[\ln\left(\frac{8R}{a}\right) - \beta\right], \tag{4}$$

where parameter β depends on the core models; for viscous cores it is 0.558 while for solid rotating cores it is 0.25. It should be mentioned that the velocity of translation of the vortex ring, V, in the simple form of Eq. (4) is obtained by connecting Lamb's equations for the impulse P and kinetic energy E through Hamilton's equation ($V = \partial E/\partial P$) assuming that core of the vortex ring is circular and ω/r is uniform inside it, where ω is azimuthal vorticity [9]. Expressions obtained for the impulse, kinetic energy, and translation velocity of the vortex ring contain an error term in the order of $O(a^2/R^2)$; hence, the condition $a/R \ll 1$ is essential. See Pedley [5] and Sullivan *et al.* [7] for more details on derivation of Eq. (4).

[*]vaselb@uwindsor.ca
[†]rupp@uwindsor.ca
[‡]dting@uwindsor.ca
[§]Stewart.Turner@anu.edu.au

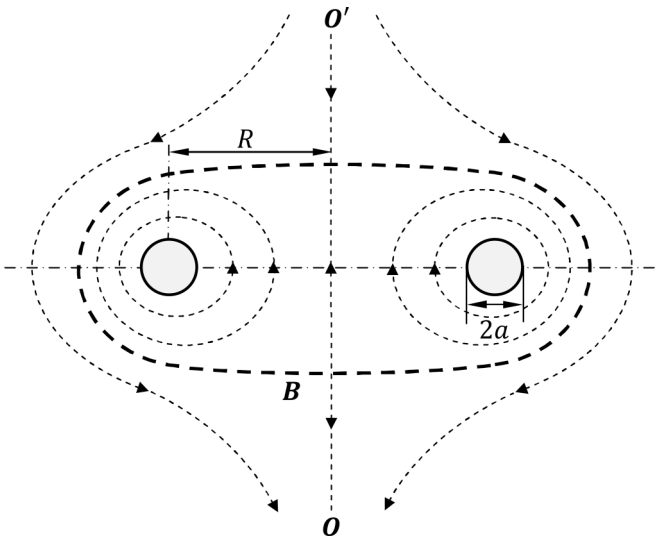

FIG. 1. Schematic sketch of a cross section through center of a vortex ring; B is the boundary of the bulk fluid carried along with the vortex ring; within this region flow is rotational whereas the ambient flow is irrotational. The shape of the boundary B depends on the ratio R/a where R and a respectively represent the ring and core radii; at $R/a < 14$, it looks like an oblate spheroid, as R/a increases points u and l approach each other and eventually meet at $R/a = 86$ forming a toroidal region.

Combining Eq. (2) with Eqs. (3) and (4) yields the following nonlinear nonhomogeneous differential equation

$$\frac{dR}{dt} = -C_1 \frac{\left[\ln(C_2 R\sqrt{R}) - \frac{1}{4}\right]^2}{R^2\sqrt{R}} + \frac{C_3}{R} \tag{5a}$$

$$R(0) = R_0, \tag{5b}$$

where $C_1 = \sqrt{6}\Gamma C_d/48\sqrt{\pi^5}$, $C_2 = 4\sqrt{6\pi}$ and $C_3 = F_B/2\pi\Gamma$. Equation (5b) is the initial condition for Eq. (5a). All parameters appearing in Eq. (5) including those with dimensions of length, time, velocity, circulation, and force are normalized using r_0, $(r_0/g)^{1/2}$, $(gr_0)^{1/2}$, $(gr_0^3)^{1/2}$, and $\rho g r_0^3$ respectively, where ρ is the density of water, g is the gravitational acceleration, and r_0 is equal to the radius of a perfect sphere enclosing the same volume of air as the initial toroidal bubble. In our recent study [6], basic scaling was used as a preliminary analysis to qualify the solution of Eq. (5a) by estimating the order of magnitude of each term. In the present letter, we propose a semianalytical solution to this equation using a perturbation technique. This solution introduces a first-order perturbation modification to Turner's radius. It is noteworthy to mention that the modifying term includes the unknown drag coefficient. Substituting the experimentally measured radius into the proposed equation yields the drag coefficient of the associated buoyant vortex ring.

II. MODEL

Considering coefficient C_1 in Eq. (5a) as the perturbation parameter, i.e., $\epsilon = C_1$, radius R can be represented by the following expansion in the first-order approximation

$$R = \Re_0 + \epsilon\Re_1 + O(\epsilon^2), \tag{6}$$

where $\Re_0$ is the zeroth-order solution and $\epsilon\Re_1$ is the first-order perturbation correction. Substituting Eq. (6) into Eqs. (5a) and (5b), expanding the resulting equations in a power series of ϵ through Taylor series, and equating to zero the terms of zeroth- and first-order in ϵ yields two sets of simpler equations as

$$\frac{d\Re_0}{dt} = \frac{C_3}{\Re_0} \tag{7a}$$

$$\Re_0(0) = R_0 \tag{7b}$$

and

$$\frac{d\Re_1}{dt} + \frac{C_3}{\Re_0^2}\Re_1 = -\frac{[\ln(C_2\Re_0\sqrt{\Re_0}) - 0.25]^2}{\Re_0{}^2\sqrt{\Re_0}}, \tag{8a}$$

$$\Re_1(0) = 0. \tag{8b}$$

Note that all terms including second- and higher-order in ϵ are neglected. Equations (7b) and (8b) are initial conditions for Eqs. (7a) and (8a) respectively. Solving Eq. (7a), the zeroth-order solution is $\Re_0 = (I_1 + 2C_3 t)^{1/2}$. By substituting $C_3 = F_B/2\pi\Gamma$ and implementing the initial condition given by Eq. (7b), we obtain

$$\Re_0 = \left(R_0^2 + \frac{F_B t}{\pi\Gamma}\right)^{1/2}. \tag{9}$$

Equation (9) is Turner's radius; i.e., $\Re_0 = R_T$. Substituting Eq. (9) into Eq. (8a), and solving Eq. (8a) using the initial condition given by Eq. (8b) gives

$$\Re_1 = -\frac{1907}{250}\frac{t}{R_T}. \tag{10}$$

It should be indicated that the term $[\ln(C_2\Re_0\sqrt{\Re_0}) - 0.25]^2$ was simply curve fitted with $[7.755\Re_0^{0.75}]$. The goodness of the curve fitting was evaluated through coefficient of determination defined as $1\text{-}SS_{\text{res}}/SS_{\text{tot}}$, where SS_{res} and SS_{tot} are the sum of squares of residuals and the total sum of squares respectively. A fairly good value of 0.9947 was obtained for the coefficient of determination in the range of $1 \leqslant R \leqslant 5$, i.e., the fit explains 99.47% of the total variation in the data about the average. The value of the coefficient of determination decreases as radius R grows beyond 5, i.e., radius of vortex ring exceeds five times r_0, which is unlikely since the vortex ring is expected to break down into small spherical-cap bubbles before reaching that point (see Cheng *et al.* [10]). It is worth noting that without the proposed curve fitting we cannot find any general solution for Eq. (8). Solving Eq. (9) for t and substituting into Eq. (10) yields

$$\Re_1 = -\frac{1551}{200}\frac{1}{2C_3}R_T\left[1 - \left(\frac{R_0}{R_T}\right)^2\right], \tag{11}$$

therefore,

$$\epsilon\Re_1 = -\Lambda\left[1 - \left(\frac{R_0}{R_T}\right)^2\right]R_T, \tag{12}$$

where $\Lambda = \alpha\Gamma^2 C_d/F_B$ in which $\alpha = 0.0711$ is a constant and C_d, as yet unknown, stands for the drag coefficient. Substituting Eqs. (9) and (12) into Eq. (6), we obtain

$$R = R_T - \Lambda\left[1 - \left(\frac{R_0}{R_T}\right)^2\right]R_T. \tag{13}$$

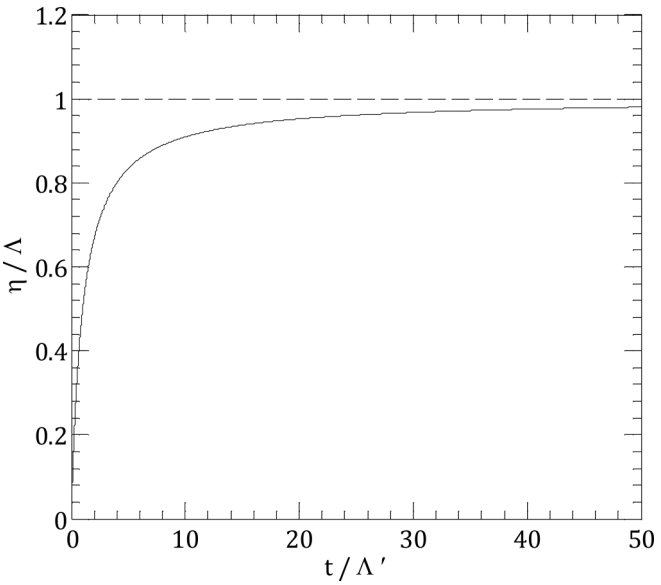

FIG. 2. Time history of the ratio of the viscous term to the buoyant term; $\Lambda = \alpha\Gamma^2 C_d/F_B$ and $\Lambda' = R_0\pi\Gamma/F_B$. The effect of the viscous term increases with time.

Accordingly, the radius of the buoyant vortex ring R includes two terms; the first term, R_T, represents the effect of the buoyancy and the second term, $\Lambda[1-(\frac{r_0}{R_T})^2]R_T$, describes the effect of the viscosity. Eq. (13) indicates that the Turner's radius overestimates the actual radius of buoyant vortex rings since it does not take into account the viscous dissipation. In fact, the viscous force causes the rate of expansion to decrease, since it acts downward in the opposite direction of the buoyant force. It is noteworthy to mention that it is not possible to plot Eq. (13) since it depends on the unknown drag coefficient—where this coefficient must be produced using Eq. (13) itself by way of the measured radius. To enable a closer comparison of the effect of viscosity with the effect of buoyancy we define parameter η as the ratio of the viscous term to the buoyant term as

$$\eta = \Lambda\left[1-\left(\frac{R_0}{R_T}\right)^2\right]. \tag{14}$$

Figure 2 illustrates the variation of η with respect to time. As is observed, the ratio of the viscous term to the buoyancy term increases asymptotically to $\Lambda = \alpha\Gamma^2 C_d/F_B$ as the vortex ring rises, i.e., viscous force becomes more considerable with time. This can be attributed to the diffusion of the vorticity generated on the vortex ring surface through the rotational area, and probably, over its boundary $\boldsymbol{B}$ sweeping off into the initially irrotational region (see Fig. 1). In Fig. 2, the value of Λ is still unknown, since the drag coefficient C_d of the vortex ring cannot be calculated through pure analytical analysis. Solving Eq. (13) for Λ, we obtain

$$\Lambda = \frac{1-\frac{R}{R_T}}{1-\left(\frac{R_0}{R_T}\right)^2}. \tag{15}$$

To determine the value of Λ we need to conduct experiments and measure the radius of the vortex ring. Plugging the measured radius R into Eq. (15) yields Λ; consequently, the drag coefficient C_d can be deduced since $\Lambda = \alpha\Gamma^2 C_d/F_B$, and so $C_d = \Lambda F_B/\alpha\Gamma^2$.

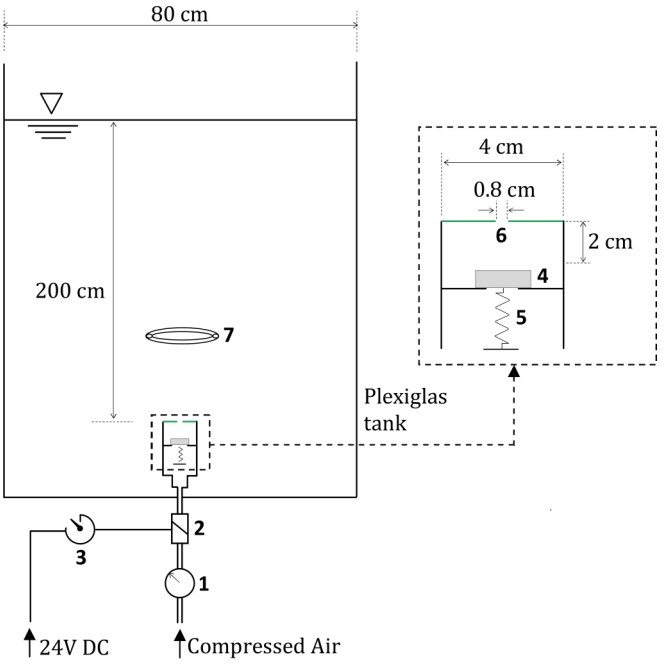

FIG. 3. (Color online) Apparatus: (1) pressure regulator, (2) solenoid valve, (3) PLC, (4) cap, (5) spring, (6) small opening on a membrane, (7) vortex ring.

III. EXPERIMENT

The experiment reported in this study was conducted in a water-filled Plexiglass tank that was 0.8 m long, 0.8 m wide, and 2.4 m high. The experimental setup is sketched in Fig. 3. As illustrated in this figure, compressed air passes through a pressure regulator (1) to a solenoid valve (2). The solenoid valve is controlled by a programmable logic controller (PLC) (3). Over a short period of time δt, the PLC opens the solenoid valve and air flow pushes the cap (4) against the force of the spring (5). Once the cap is lifted, pressurized air bursts out through the small opening on the flexible membrane (6) and produces an air-core vortex ring (7) inside the water. Similar to Hershberger *et al.* [8], all the experimental data were obtained photographically. Three cameras with speed of 60 f.p.s. at a resolution of 1080P were configured above and on two orthogonal sides of the tank to record the generation and the motion of the vortex ring bubble. The videos were then analyzed frame by frame using the MATLAB image processing tool bar to deduce the time history of the elevation and dimensions of the vortex ring bubble. The rise velocity V was obtained as the first derivative of measured elevation. Substituting the rise velocity and the dimensions of the vortex ring bubble into Eq. (4) yields circulation as

$$\Gamma = 4\pi RV\left[\ln\left(\frac{8R}{a}\right)-\beta\right]^{-1}. \tag{16}$$

It is worth mentioning that in the paper of Turner [2], which was the forerunner of the present work, dyed buoyant fluid was injected into a tank of water. The density difference was small,

and the viscosity difference negligible. In strong contrast, for the experiments described in the present paper, a pulse of air is impulsively injected into water, forming an air-core vortex ring. This has a large density and viscosity difference from water, and there is also surface tension across the interface. Each of these has a substantial influence on the behavior of the air-core vortex and together they produce the drag, which is the subject of this paper.

IV. RESULTS AND DISCUSSION

The vortex ring is characterized by the reciprocal of dimensionless surface tension, the Bond number, given as $\mathrm{Bo} = \rho g {r_0}^2 / T$, where T is the water-air surface tension. Using the experimental setup described in Fig. 3, the Bond number of the vortex ring can be controlled by the inlet pressure of the air flow, the duration of release through the solenoid valve, the diameter of the opening and the height of water over the vortex ring generator. The vortex ring bubble studied herein was generated at a supplied pressure of 20 psi (almost 138 kPa) over a duration of 0.1 s while the diameter of the opening was 0.08 m and the height of water over the membrane was set to be 1.5 m, leading to a Bond number of 85 ± 5. It should be mentioned that the air-water surface tension was assumed to be $T = 72.8 \times 10^{-5}\mathrm{N\ cm^{-1}}$ since water temperature was approximately 20 °C during the experiment. The given precision uncertainty was obtained from the standard deviation of ten individual measurements at a 95% confidence level.

Figure 4 attempts to illustrate the formation and translation of the buoyant vortex ring corresponding to $\mathrm{Bo} = 85$. Figure 4(a) represents the approximate moment that the pressurized air burst out through the small opening on the flexible membrane (green surface); Fig. 4(b) corresponds to the moment at which the vortex ring was formed; and Fig. 4(h) depicts the vortex ring at the moment that the free surface started to bow; beyond this moment the vortex ring would be affected by the free surface (free surface is not shown in the figure).

As is clearly observed in Fig. 4, the buoyant vortex ring expands radially as it rises. The time history of the radius of this vortex ring bubble is plotted in Fig. 5. To ensure the negligibility of the free surface tension, the radius was not measured beyond $t = 50$. Although the experiment was carefully controlled to minimize the uncertainties, the repeatability was assessed by estimating the precision of individual measurements. Error bars shown in Fig. 5 represent precision of ten individual measurements at a 95% confidence level. Figure 5 compares the experimentally observed radius with that predicted by the Turner's equation [Eq. (1)]. As is observed, the radius calculated through the Turner's equation R_T is greater than that obtained experimentally R, and the disparity increases as the vortex ring bubble rises. This overestimation was already predicted by Eq. (13). According to Eq. (13), the actual radius of a buoyant vortex ring R equals to Turner's radius R_T minus the quantity $\Lambda[1 - (\frac{R_0}{R_T})^2]R_T$. Accordingly, the difference between the Turner's radius and the one measured experimentally, i.e., $\Lambda[1 - (\frac{R_0}{R_T})^2]R_T$, is directly related to the viscous effect, since $\Lambda = \alpha\Gamma^2 C_d / F_B$ and C_d represents the effect of viscosity. As time goes by, the vorticity produced on the surface of the vortex ring diffuses through the ambient flow; consequently, the effect of viscosity becomes more noticeable ($F_{\mathrm{viscous}} = \nu\nabla \times \omega$), and the measured values diverge from the radii reported by Turner.

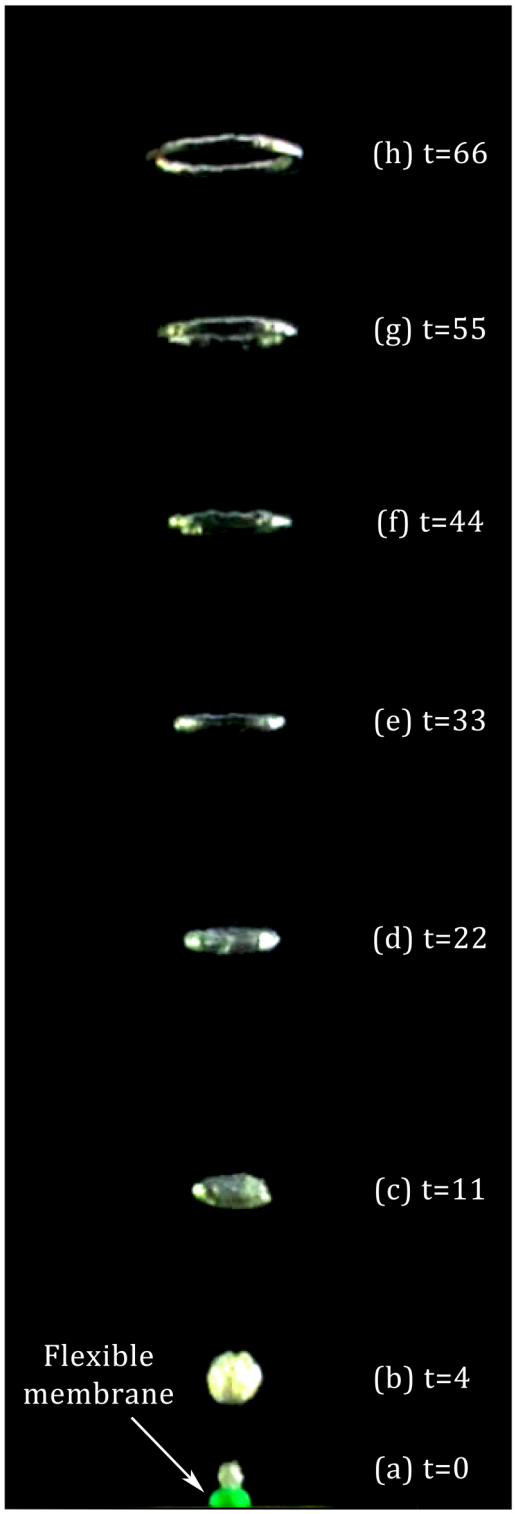

FIG. 4. (Color online) Formation and translation of the vortex ring bubble corresponding to Bo = 85. Values are dimensionless.

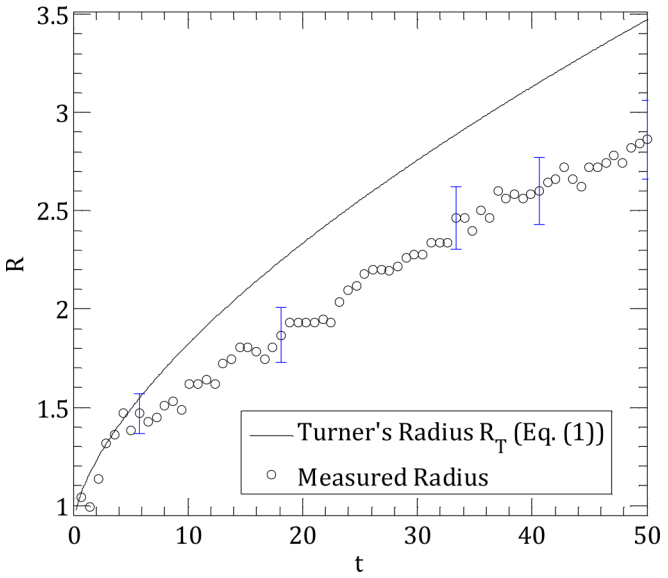

FIG. 5. (Color online) Radius of a buoyant vortex ring at Bo = 85; values are dimensionless. Solid line shows Turner's radius [Eq. (1)] and circles represent measured values.

The time history of the circulation associated with the vortex ring described in Fig. 5 is illustrated in Fig. 6. The data presented in this figure is calculated using Eq. (16) assuming a solid rotating core (i.e., $\beta = 0.25$). It can be seen that circulation is approximately constant with respect to time with an average value of 6.54—which is consistent with experiments conducted by Walters and Davidson [4]. Here it is noteworthy to mention again that the circulation and all other parameters have been made dimensionless using terms explained below Eq. (5). Substituting the Turner's and measured radii reported in Fig. 5 into Eq. (15) yields

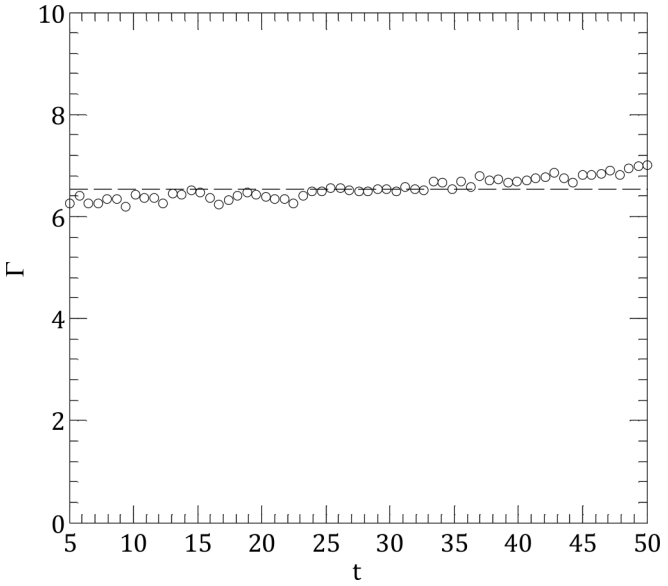

FIG. 6. Circulation of a buoyant vortex ring at Bo = 85; values are dimensionless. Dashed line shows the average circulation of approximately 6.54.

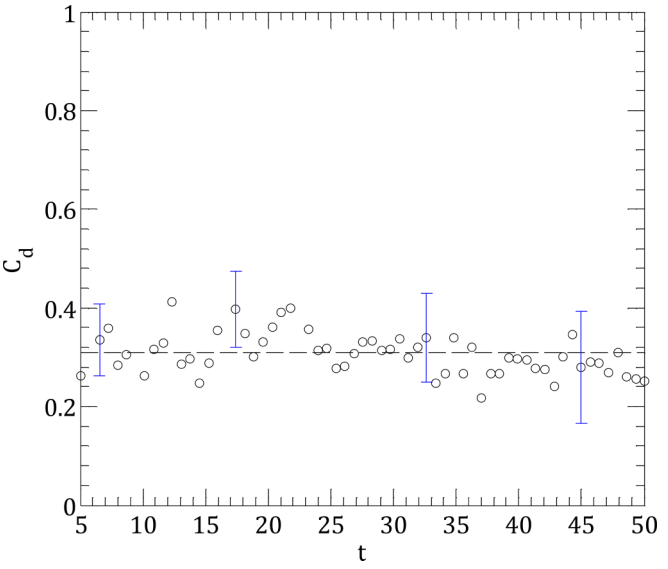

FIG. 7. (Color online) Drag coefficient of a buoyant vortex ring at Bo = 85; values are dimensionless. Dashed line shows the average drag coefficient of approximately 0.31.

$\Lambda = \alpha\Gamma^2 C_d/F_B$, then, using circulation given in Fig. 6 the drag coefficient of the buoyant vortex ring was deduced as shown in Fig. 7. We observe that the time history of the drag coefficient is approximately constant with a relative standard deviation of 12% and an average value of $C_d = 0.31$.

V. CONCLUSION

In the present paper, a semianalytical method was proposed to compare the effect of viscosity with the effect of buoyancy on the radial expansion of buoyant vortex rings. Applying the proposed method along with the flow visualization enables us to deduce the drag coefficient of buoyant vortex rings. To demonstrate the proposed hybrid technique, the drag coefficient of a vortex ring bubble at a Bond number of approximately 85 was calculated. First, the vortex ring bubble was experimentally visualized and the ring radius was measured by photography. Second, the circulation of the vortex ring bubble was calculated through Eq. (16). Substituting the measured radius into Eq. (15), we obtained Λ. Following this, the drag coefficient was deduced using $C_d = \Lambda F_B/\alpha\Gamma^2$. The same procedure can be applied to determine the drag coefficient of vortex ring bubbles generated through other mechanisms—for instance, using a vortex gun or a balloon bursting underwater—at other Bond numbers and fluid viscosities.

ACKNOWLEDGMENTS

Authors are deeply indebted to Professor M. Cheng for generously providing them with his vortex ring generator details. This research has been funded by the Natural Sciences and Engineering Research Council of Canada and the Ontario Trillium Foundation.

[1] L. Gan, J. R. Dawson, and T. B. Nickels, On the drag of turbulent vortex rings, J. Fluid Mech. **709**, 85 (2012).

[2] J. S. Turner, Buoyant vortex rings, Proc. R. Soc. A **239**, 61 (1957).

[3] T. S. Lundgren and N. N. Mansour, Vortex ring bubbles, J. Fluid Mech. **224**, 177 (1991).

[4] J. K. Walters and J. F. Davidson, The initial motion of a gas bubble formed in an inviscid liquid, J. Fluid Mech. **17**, 321 (1963).

[5] T. J. Pedley, The toroidal bubble, J. Fluid Mech. **32**, 97 (1968).

[6] A. R. Vasel-Be-Hagh, R. Carriveau, and D. S.-K. Ting, A balloon bursting underwater, J. Fluid Mech. **769**, 522 (2015).

[7] I. S. Sullivan, J. J. Niemela, R. E. Hershberger, D. Bolster, and R. J. Donnelly, Dynamics of thin vortex rings, J. Fluid Mech. **609**, 319 (2008).

[8] R. E. Hershberger, D. Bolster, and R. J. Donnelly, Slowing of vortex rings by development of Kelvin waves, Phys. Rev. E **82**, 036309 (2010).

[9] H. Lamb, *Hydrodynamics* (Cambridge University Press, Cambridge, 1916), pp. 231–232.

[10] M. Cheng, J. Lou, and T. T. Lim, Motion of a bubble ring in a viscous fluid, Phys. Fluids **25**, 067104 (2013).